

TRANSITION METAL COMPLEXES PRODUCED FROM DIPICOLINIC ACID: SYNTHESIS, STRUCTURAL CHARACTERIZATION, AND ANTI-MICROBIAL INVESTIGATIONS

Prakash Kumar Sahoo¹, Susanta Kumar Biswal^{1*} and Mohammad Azam^{2*}

¹Department of Chemistry, Centurion University of Technology and Management, Odisha, India

²Department of Chemistry, College of Science, King Saud University, Riyadh PO BOX 2455, Riyadh 11451, Saudi Arabia

Received June 29, 2021; Revised June 9, 2022; Accepted June 10, 2022

ABSTRACT. A novel series of mononuclear complexes of the type, $[M(L)(H_2O)_2]$ [$M = Co(II)$ (1), $Ni(II)$ (2), $Zn(II)$ (3), $Cd(II)$ (4), $L =$ dipicolinate), has been investigated using various techniques, including elemental analyses, FT-IR, ¹H- and ¹³C NMR spectroscopy, powder XRD and thermogravimetric analysis. The results indicate that the coordination of the dipicolinic acid to the metal ions involves two carboxylate O atoms, the pyridine N atom, and two water molecules. The pyridine-2,6-dicarboxylic acid and its studied compounds have been screened against microbial species. The findings show that the complexes have higher activity in comparison to the free pyridine-dicarboxylic acid.

KEY WORDS: Dipicolinic acid, Metal complexes, Antimicrobial activity

INTRODUCTION

Pyridine-2,6-dicarboxylic acid has been proven to have a broad range of biological uses in medicine and pharmaceuticals, as well as a significant function in coordination chemistry and catalysis [1-3]. Pyridine-2,6-dicarboxylic acid, also known as dipicolinic acid (DPA), acts as a versatile multidentate ligand and forms stable complexes of a limited steric hindrance with various metals ions via two carboxyl oxygen atoms situated at 120° angle and pyridine ring nitrogen atom, providing interesting topologies and physical properties, such as the photoluminescence, gas adsorption, catalysis, multifunctional materials and nonlinear optics under the appropriate conditions [1-11]. Furthermore, DPA-based complexes act as electron carriers in various biological systems as specific molecular tools in DNA cleavage and NO scavenging [3, 12]. Therefore, various experimental and theoretical studies have been carried out using pyridine-2,6-dicarboxylic acid due to the importance of intramolecular proton transfer in many chemical and biological reactions [12-15]. Furthermore, DPA ligands are found in a variety of natural compounds, produced from the oxidative degradation of vitamins, coenzymes, and alkaloids [12]. In particular, the pyridine-2,6-dicarboxylic acid analog, commonly known as dipicolinic acid, is a useful ligand system to mimic possible pharmaceutically active molecules because of its low toxicity, amphiphilic nature, and wide range of biological activity [15-17]. Therefore, taking into account the wide significance of DPA, we are reporting here a series of mononuclear metal complexes derived from DPA with $Co(II)$ (1), $Ni(II)$ (2), $Zn(II)$ (3), and $Cd(II)$ (4) ions. The synthesized compounds were investigated using elemental analyses, FT-IR, TGA, and NMR studies. In addition, the free DPA and its complexes with metal ions were also tested for *in vitro* antimicrobial activity. The results show that the metal complexes have significant antimicrobial properties in comparison to free DPA.

*Corresponding author. E-mail: dr.skbiswal@cutm.ac.in (SKB), azam_res@yahoo.com (MA)
This work is licensed under the Creative Commons Attribution 4.0 International License

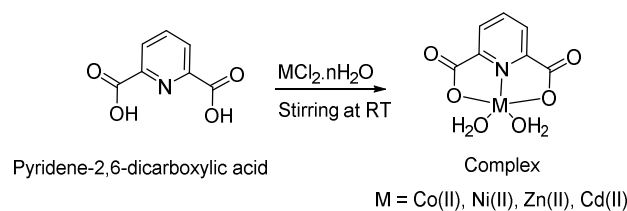
EXPERIMENTAL

Chemicals and methods

All chemicals used in this experiment were of AR grade and used as received. Hydrated metal chlorides, pyridine-2,6-dicarboxylic acid (Aldrich) were used as received. FT-IR spectra recorded at the range 400-4000 cm^{-1} were obtained using the Perkin Elmer 621 spectrophotometer using KBr as a disc pallet. The microanalyses were performed on Elementar Vario elemental analyzer. The NMR (^1H - and ^{13}C) were recorded in Jeol spectrometer at 400 and 100 MHz, respectively in d_6 -DMSO. The thermogravimetric analyses were carried out in the inert atmosphere of nitrogen.

General procedure for the synthesis of complexes

$\text{MCl}_2 \cdot n\text{H}_2\text{O}$ was added to an alcoholic solution of pyridine-2,6-dicarboxylic acid (50 mg, 3.0 mmol) in an equal molar ratio. The reaction mixture was stirred for 5 h, which led to the formation of a colored precipitate (Scheme 1). The isolated product was washed subsequently with ether and hexane and dissolved in the mixture of deionized water and ethanol to obtain an analytically pure compound.



Scheme 1. Schematic representation of designed complexes.

Antimicrobial studies

Pyridine-2,6-dicarboxylic acid and its metal complexes were tested for *in-vitro* antimicrobial activity against bacterial species, *P. aeruginosa*, *S. sonnei*, *E. coli* and fungal species, *Aspergillus niger*, *A. flavus*, *F. oxysporum*, *Candida albicans* using the Kirby Bauer Disc diffusion method using agar nutrient as the medium [18]. Amoxicillin (30 $\mu\text{g}/\text{disc}$) and Fluconazole (30 $\mu\text{g}/\text{disc}$) were used as the standard antibacterial and antifungal drugs, whereas the DMSO was considered a negative control in the experiment. To perform the Kirby-Bauer disk diffusion assay, the test agar plate swabbed with a standardized concentration of the test organism was developed, and then filter paper with defined antibiotic concentration was immersed into the petri-dish. The titled complexes were dissolved in DMSO (50 $\mu\text{g}/\text{mL}$), and then, a thick filter paper disc was immersed in the solution. The prepared discs with title complexes were again immersed into the petri-dish possessing the test organism and incubated at a standard temperature of 37 $^\circ\text{C}$. After incubating bacterial and fungal species for 24 h and 72 h, respectively, the diameter of the zone of inhibited growth caused by each of the title complexes was measured (Table 1). The MIC for the title complexes was measured by the broth micro-dilution method by means of 96 well microtitration plates against bacterial and fungal species [19-20].

The MIC of each tested title complex against bacterial (10^5 CFU mL^{-1}) and fungal (10^5 CFU mL^{-1}) species was evaluated by inoculating in DMSO in the varying concentration. In brief, the MIC is the lowest concentration of the title complex to restrict the observable growth of bacterial and fungal species at 37 $^\circ\text{C}$ after the incubation of 24 h and 48 h, respectively. The MIC and zone

of inhibition (IZ) of the tested compounds against the studied bacterial and fungal species at standard temperatures of 37 °C and 24 h and 48 h incubation are given in Table 1.

Table 1. Inhibition zones (mm) and minimum inhibitory concentration (MIC) caused by synthesized compounds against microbial strains.

Microbial test strains	Inhibition zone (mm)/MIC ($\mu\text{g/mL}$)					Inhibition zone/MIC ($\mu\text{g/mL}$)	
	L	1	2	3	4	Amoxicillin	Fluconazole
<i>P. aeruginosa</i>	8/500	21/61.5	14/120	12/120	11/120	25/11.5	
<i>E. coli</i>	7/500	16/125	13/120	11/120	13/120	28/22	
<i>S. sonnei</i>	8/500	20/61.5	15/120	17/120	15/120	25/120	
<i>A. niger</i>	12/500	22/120	21/120	23/120	16/120		25/60.5
<i>A. flavus</i>	11/500	23/120	21/120	22/120	18/120		20/120
<i>F. oxysporum</i>	12/500	16/120	18/120	24/120	13/120		18/120
<i>C. albicans</i>	9/500	18/120	16/120	22/120	15/120		18/120

RESULTS AND DISCUSSION

The FT-IR spectra in all the complexes are characterized by the absence of a band near 3000–3450 cm^{-1} , suggesting the deprotonation of carboxylate groups in the complexes (Figure 1) (Table 2) [21, 22]. Furthermore, the characteristic sharp bands near 1600–1625 cm^{-1} and 1365–1370 cm^{-1} are accredited to the asymmetric (ν_{as}) and the symmetric (ν_{s}) stretching vibrations of the COO groups [14, 22–23]. However, the difference in the peak values of asymmetric and symmetric vibrations indicates the monodentate coordination of the carboxylic groups to metal ions [14, 22–23]. In addition, the weak aromatic C-H stretching vibrations appear near 3050 cm^{-1} in all the title complexes [22, 24–25]. In addition, the IR spectra of the complexes reveal the presence of a wide intensity band in the high-frequency area at around 3395–3420 cm^{-1} assigned to the OH stretching vibrations of the coordinated water molecules [22, 24, 26].

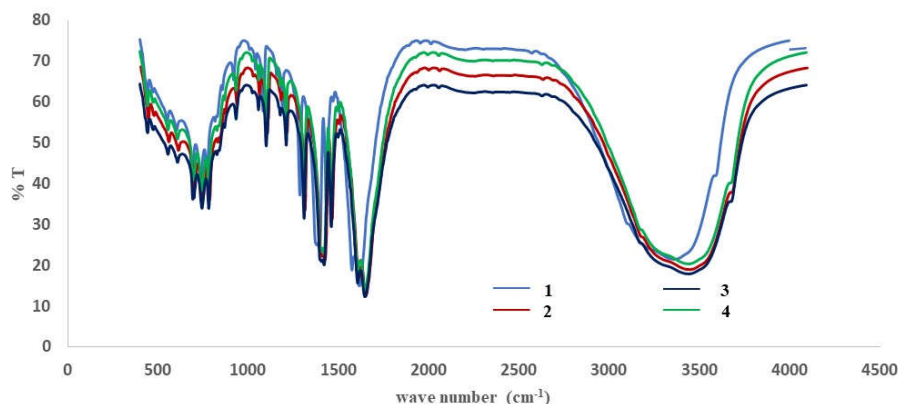
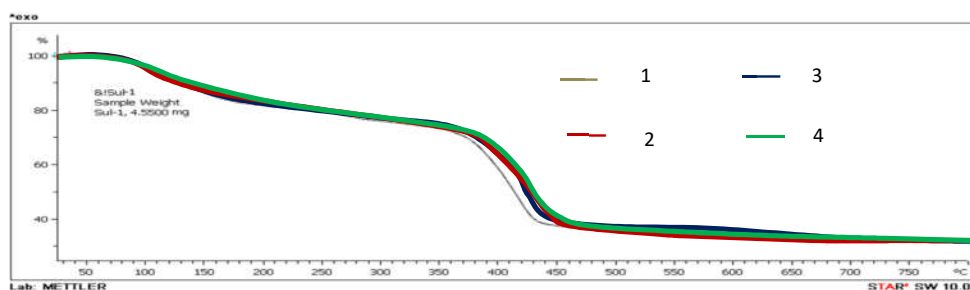


Figure 1. IR spectra of complexes 1, 2, 3 and 4.

Table 2. Physicochemical studies for complexes **1**, **2**, **3** and **4**.

Complexes	FW	Anal Cal (Found) in %			IR (KBr, cm ⁻¹)
		C	H	N	
Complex 1 C ₇ H ₇ CoNO ₇	260.07	32.33 (32.25)	2.71 (2.68)	5.39 (5.35)	1625, 1370
Complex 2 C ₇ H ₇ NNiO ₆	259.83	32.36 (32.35)	2.72 (2.68)	5.39 (5.35)	1600, 1365
Complex 3 C ₇ H ₇ NO ₆ Zn	266.51	31.55 (31.48)	2.65 (2.59)	5.26 (5.19)	1620, 1367
Complex 4 C ₇ H ₇ CdNO ₆	313.15	26.81 (26.76)	2.25 (2.18)	4.47 (4.41)	1623, 1369

Figure 2. TG spectra of complexes **1**, **2**, **3** and **4**.

The thermogravimetric analysis was investigated to understand the decomposition pattern of the studied mononuclear complexes in the inert atmosphere of nitrogen and revealed a two-step decomposition pattern. The first degradation peak observed at 160 °C was accompanied by the release of two coordinated water molecules, corresponding to a mass loss of ~13.80% of the complex. The second thermolytic step which begins at 390 °C and ends at about 360 °C, brings the expulsion of the whole organic moiety, consistent with ~ 64.37% mass loss of the complex

NMR spectroscopy

The ¹H-NMR spectrum reveals multiplet corresponding to aromatic protons at 7.60-7.69 ppm (3H, m, Ar-H). The ¹³C-NMR spectrum of complex **3** reveals signals due to aromatic carbons at 129.1, 132.0, and 132.2 ppm, whereas the carboxylate carbon signal appears at 167.4 ppm, thus confirming the proposed structure for the complex (Figure 3). Similarly, complex **4** has a carboxylate signal at 165.5 ppm and aromatic carbon signals at 148.1, 128.4 and 126.8 ppm, ascertaining the proposed structures for the complex **4** (Figure 4).

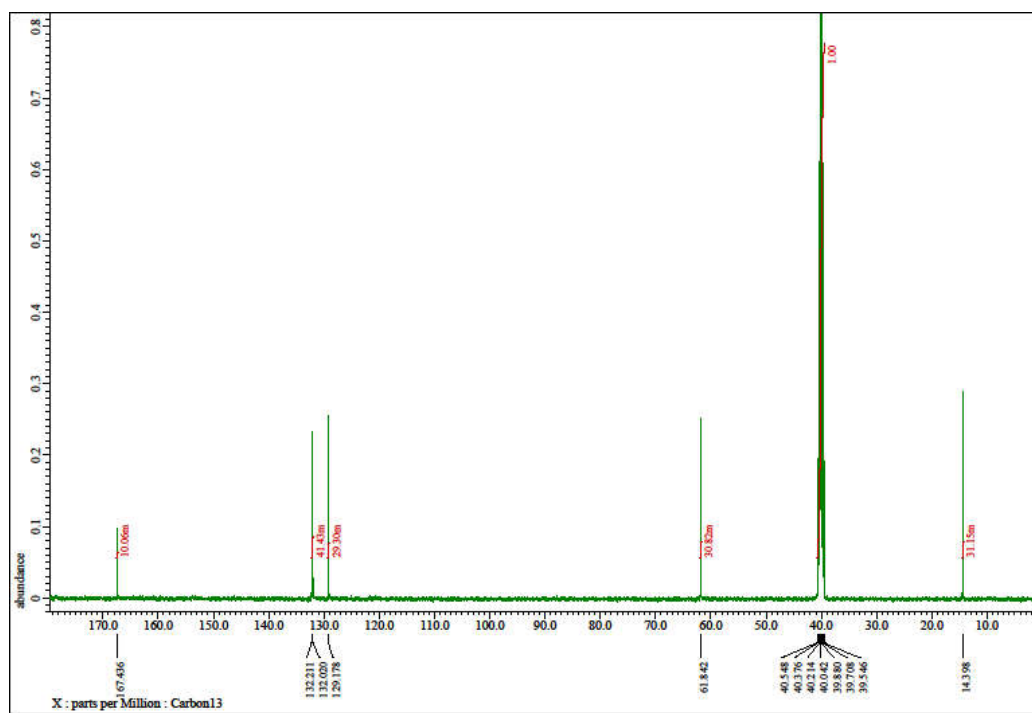


Figure 3. ^{13}C NMR spectrum of complex **3**.

PXRD

The powder XRD patterns were used to investigate the crystalline structures of complex **2** on a Bruker D2 Phaser X-ray diffractometer with $\text{CuK}\alpha$ radiation ($\lambda = 1.5418$), accelerating voltage and current of 30 kV and 10 mA, respectively, (Bruker, Berlin, Germany) at a wavelength of 1.5406 Å and 2θ range of 0° - 90° . The findings revealed that the complexes under investigation showed well-defined sharp crystalline peaks, indicating high crystallinity. We only show the diffractogram of complex **2** (Figure 5) because all of the complexes have a similar structure. Bragg's equation $n\lambda = 2d\sin\theta$ was used to calculate the maximum reflection at $2\theta = 29.74$ and inter-planar distance at $d = 3.00$ Å. The average crystallite size for the complexes was measured using Scherrer's formula [26], and it ranged between 31.0 - 51.0 nm.

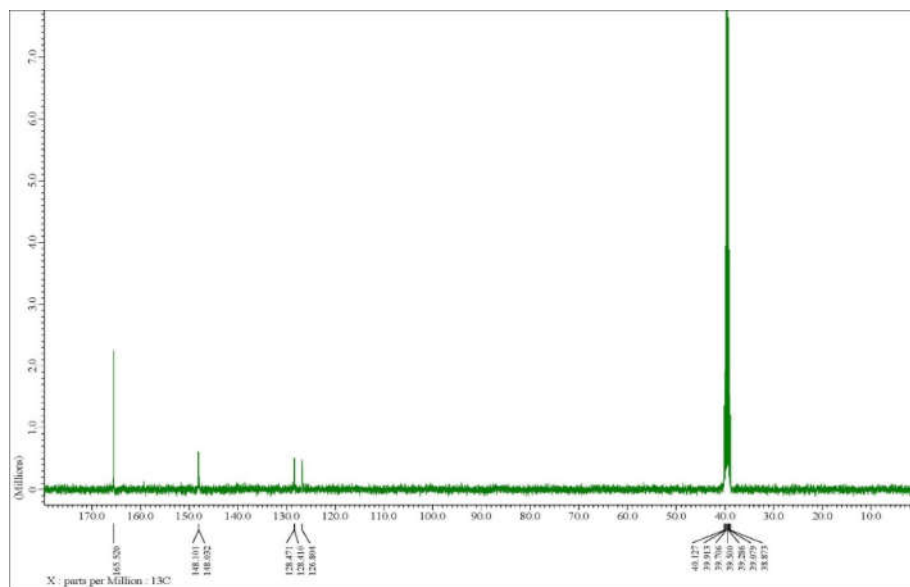
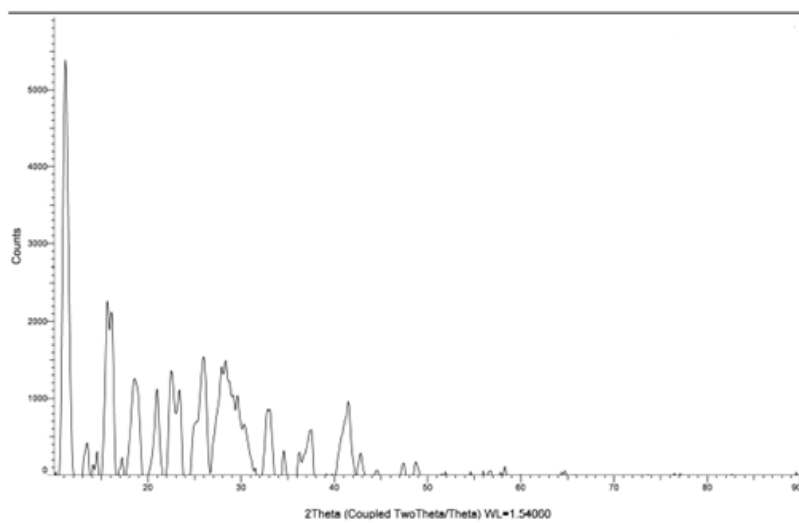
Figure 4. ^{13}C NMR spectrum of complex 4.

Figure 5. Diffractogram of complex 2.

Antibacterial and antifungal activity analysis

The antimicrobial data given in Table 1 suggests py-2,6-DCA to be less antimicrobial agent in comparison to its synthesized complexes **1-4** against the tested microbial species. However, this can be better explained by the Tweedy's chelation theory, which reveals that the binding of the ligand to metal ion decrease the polarity of the metal ion within the chelate ring system, thus causing the increase in the lipophilicity of the complexes, which later favors the permeation into the lipid layers of the bacterial cell membrane [28, 29].

To calculate the antimicrobial activity, the diameters of zone of inhibition around ligand and its complexes was measured. Antimicrobial results in comparison to the reference drug are illustrated in Table 1, and suggest the different zone of inhibition for various studied complexes against tested microbial species. The studied complex **1** and **4** show moderate antibacterial activity against *S. sonnei*, *B. subtilis* and *P. aeruginosa* pathogens with inhibition zone/MIC 20 mm/61.5 µg/mL, 28 mm/12.5 µg/mL and 21/61.5 µg/mL on comparing with standard drug Amoxicillin (Table 1). However, the complex **1** and **3** bring retardation in the growth of fungal species *A. flavus*, *A. niger*, and *P. notatum* and expand the zone of inhibition 23 mm (120 µg/mL), 23 mm (120 µg/mL) and 2 mm (120 µg/mL), respectively, and suggest the significant antifungal activity with reference to the standard drug Fluconazole.

CONCLUSION

We successfully investigated a novel series of complexes derived from pyridine-2,6-dicarboxylic acid using elemental analyses and various spectroscopic studies. Studies reveal that the coordination of py-2,6-dicarboxylate ion to the metal ion occurs via two carboxylate oxygen atoms, one pyridine N atom and two water molecules. All the investigated complexes, including py-2,6-dicarboxylic acid, were tested *in-vitro* for antimicrobial activity. In comparison to the free py-2,6-dicarboxylic acid, the complexes show to be effective antimicrobial agent.

ACKNOWLEDGEMENT

The authors acknowledge the financial support through Researchers Supporting Project number (RSP-2021/147), King Saud University, Riyadh, Saudi Arabia.

REFERENCES

1. Das, B.; Baruah, J.B. Coordinated cations in dipicolinato complexes of divalent metal ions. *Inorg. Chim. Acta*, **2010**, 363, 1479-1487.
2. Ghosh, S.K.; Ribas, J.; Bharadwaj, P.K. Metal-organic framework structures of Cu(II) with pyridine-2,6-dicarboxylate and different spacers: identification of a metal bound acyclic water tetramer. *CrystEngComm*. **2004**, 6, 250-256.
3. Naik, J.L.; Reddy, B.V.; Prabavathi, N. Experimental (FTIR and FT-Raman) and theoretical investigation of some pyridine-dicarboxylic acids. *J. Mol. Struct.* **2015**, 1100, 43-58.
4. Ay, B., Dogan, N., Yildiz, E.; Kani, I. A novel three dimensional samarium(III) coordination polymer with an unprecedented coordination mode of the 2,5-pyridinedicarboxylic acid ligand: Hydrothermal synthesis, crystal structure and luminescence property. *Polyhedron* **2015**, 88, 176-181.
5. Zhao, D.; Liu, X.-H.; Zhao, Y.; Wang, P.; Liu, Y.; Azam, M.; Al-Resayes, S.I.; Lu, Y.; Sun, W.-Y. Luminescent Cd(II)-organic frameworks with chelating NH₂ sites for selective detection of Fe(III) and antibiotics. *J. Mater. Chem. A* **2017**, 5, 15797-15807.

6. Grossel M.C.; Golden, C.A.; Gonn, J.R.; Horton, P.N.; Merckel, D.A.S.; Oszer, M.E.; Parker, R.A. Solid-state behaviour of pyridine-2,6-dicarboxylate esters: supramolecular assembly into infinite tapes. *CrystEngCommun* **2001**, *42*, 170–173.
7. Cui, G.H.; He, C.H.; Jiao, C.H.; Geng, J.C.; Blatov, V.A. Two metal–organic frameworks with unique high-connected binodal network topologies: Synthesis, structures, and catalytic properties. *CrystEngCommun* **2012**, *14*, 4210–4216.
8. Huang, Y.G.; Jiang, F.L.; Hong, M.C. Magnetic lanthanide–transition-metal organic–inorganic hybrid materials: From discrete clusters to extended frameworks, *Coord. Chem. Rev.* **2009**, *253*, 2814–2834.
9. Kukovec, B.-M.; Venter, G.A.; Olive, C.L. Structural and DFT studies on the polymorphism of a cadmium(II) dipicolinate coordination polymer. *Cryst. Growth & Des.* **2012**, *12*, 1, 456–465
10. Parveen, M.; Ghalib, R.M.; Alam, M.; Singh, M. Isolation, characterization and X-ray analysis of peltophorin from the leaves of *Peltophorum vogelianum* (Benth.). *J. Saudi Chem. Soc.* **2013**, *17*, 303–305
11. Alam, M; Park, S. Spectroscopic identifications, molecular docking, neuronal growth and enzyme inhibitory activities of steroidal nitro olefin: Quantum chemical study. *ChemSelect* **2019**, *4*, 12062–12075
12. Groves, J.T.; Kady, I.O. Sequence-specific cleavage of DNA by oligonucleotide-bound metal complexes. *Inorg. Chem.* **1993**, *32*, 3868–3872.
13. Yenikaya, C.; Buyukkidan, N.; Sari, M.; Kesli, R.; Ilkimen, H.; Bulbul, M.O.; Buyukgungor, O. Synthesis, characterization and biological evaluation of novel Cu(II) complexes with proton transfer salt of 2,6-pyridinedicarboxylic acid and 2-amino-4-methylpyridine *J. Coord. Chem.* **2011**, *64*, 3353–3365.
14. Demir, S.; Çepni, H.M.; Hołyńska, M.; Kavanoz M, Yilmaz, F.; Zorlu, Y. Copper(II) complexes with pyridine-2,6-dicarboxylic acid from the oxidation of copper(I) iodide, *J. Coord. Chem.* **2017**, *70*, 3422–3433
15. He, R.Y.; Chen, W. A novel Cd(II) coordination polymer of highly sensitive sensing for antibiotics in aqueous medium. *Polyhedron* **2022**, *221*, 115827.
16. Das, A.; Sharma, P.; Gomila, R.M.; Frontera, A.; Verma, A.K.; Sharma, B.; Barthakur, T. Synthesis, structural topologies and anticancer evaluation of phenanthroline-based 2,6-pyridinedicarboxylato Cu(II) and Ni(II) compounds. *Polyhedron* **2022**, *213*, 115632
17. Sharma, P.; Sharma, P.; Frontera, A.; Barcelo-Olive, M.; Verma, A.K.; Barthakur, T.; Bhattacharyya, M.K. Unconventional π -hole and Semi-coordination region bonding interactions directed supramolecular assemblies in pyridinedicarboxylato bridged polymeric Cu(II) Compounds: Antiproliferative evaluation and theoretical studies. *Inorg. Chim. Acta* **2021**, *525*, 120461
18. Bauer, A.W.; Kirby, W.M.M.; Sherris, J.C.; Truck, M. Antibiotic susceptibility testing by a standardized single disk method. *Am. J. Clin. Pathol.* **1966**, *45*, 493–496.
19. Wayne, P.A. *Clinical and Laboratory Standards Institute: Methods for Dilution Antimicrobial Susceptibility Tests for Bacteria That Grow Aerobically, Approved Standard*, 7th ed., CLSI Document M7-A7, **2006**, PMID: 5908210.
20. Wiegand, I.; Hilpert, K.; Hancock, R.E.W. Agar and broth dilution methods to determine the minimal inhibitory concentration (MIC) of antimicrobial substances. *Nat. Prod.* **2008**, *3*, 163–175.
21. Devereux, M.; McCann, M.; Leon, V.; McKee, V.; Ball, R.J. Synthesis and catalytic activity of manganese(II) complexes of heterocyclic carboxylic acids: X-ray crystal structures of [Mn(pyr)₂]_n, [Mn(dipic)(bipy)₂].4.5H₂O and [Mn(chedam)(bipy)].H₂O (pyr = 2-pyrazinecarboxylic acid; dipic = pyridine-2,6-dicarboxylic acid; chedam = chelidamic acid(4-hydroxypyridine-2,6-dicarboxylic acid); bipy = 2,2-bipyridine). *Polyhedron* **2002**, *21*, 1063–1071.

22. Nakamoto, K. *Infrared and Raman Spectra of Inorganic and Coordination Compounds*, 3rd ed., Wiley: New York; **1978**.
23. Zang, Q.; Zhong, G.Q.; Wang, M.L. A copper(II) complex with pyridine-2,6-dicarboxylic acid: Synthesis, characterization, thermal decomposition, bioactivity and interactions with herring sperm DNA. *Polyhedron* **2015**, 100, 223-230.
24. Azam, M.; Wabaidur, S.M.; Alam, M.J.; Trzesowska-Kruszynska, A.; Kruszynski, R.; Alam, M.; Al-Resayes, S.I.; Dwivedi, S.; Khan, M.R.; Islam, M.S. Synthesis, structural investigations and pharmacological properties of a new zinc complex with a N4-donor Schiff base incorporating 2-pyridyl ring. *Inorg. Chim. Acta* **2019**, 487, 97-106
25. Shakir, M.; Azam, M.; Azim, Y.; Parveen, S.; Khan, A.U. Synthesis and physico-chemical studies on complexes of 1,2-diaminophenyl- N, N'-bis-(2-pyridinecarboxaldimine), (L): A spectroscopic approach on binding studies of DNA with the copper complex. *Polyhedron* 2007, 26, 5513-5518
26. Shakir, M.; Shahid, N.; Sami, N.; Azam, M.; Khan, A.U. Synthesis, spectroscopic characterization and comparative DNA binding studies of Schiff base complexes derived from L-leucine and glyoxal. *Spectrochim. Acta Part A* **2011**, 82, 31-36.
27. Stepanenko, I.N.; Casini, A.; Edefe, F.; Novak, M.S.; Arion, V.B.; Dyson, P.J.; Jakupec, M.A.; Kepple, B.K. Conjugation of organoruthenium(II) 3-(1H-benzimidazol-2-yl)pyrazolo[3,4-b]pyridines and indolo[3,2-d]benzazepines to recombinant human serum albumin: A strategy to enhance cytotoxicity in cancer cells. *Inorg. Chem.* **2011**, 50, 12669-12679
28. AlResayes, S.I.; Shakir, M.; Shahid, N.; Azam, M.; Khan, A.U. Synthesis, spectroscopic characterization and in vitro antimicrobial studies of Schiff base ligand, H₂L derived from glyoxalic acid and 1,8-diaminonaphthalene and its Co(II), Ni(II), Cu(II) and Zn(II) complexes. *Arab. J. Chem.* **2016**, 9, 335-343
29. Soltani, B.; Ghorbanpour, M.; Ziegler, C.J.; Ebadi-Nahari, M.; Mohammad-Rezaei, R. Nickel (II) and cobalt (II) complexes with bidentate nitrogen-sulfur donor pyrazole derivative ligands: Syntheses, characterization, X-ray structure, electrochemical studies, and antibacterial activity. *Polyhedron* **2020**, 180, 114423.